Chapter 1
Introduction

1.1 Background and Significance

In August 2016, Chinese high-orbit satellite was successfully launched from Xichang Satellite Launch Center, realizing full coverage communication to the domestic and surrounding sea areas, making “not in the service area” no longer happen, and opening a new era of Chinese autonomous satellite telephone. In May 2018, Queqiao, Chang’e-4s relay satellite took the Long March 4C launch vehicle into the Earth-Moon transfer orbit with the perigee at about 200 km and the apogee at about 400,000 km, becoming the first special relay communication satellite outside the earth orbit in human history. The satellite antenna mounted on the Queqiao is designed with an deployable umbrella-like parabolic surface, which is folded and closed during rocket transport to save storage space, and deploys and maintains its parabolic configuration after the satellite is in orbit, with a diameter of 4.2 m after full deployment. This is a new breakthrough in the field of lunar exploration in China, and also marks that China has taken the lead in mastering the earth-moon relay communication technology.

The above-mentioned high-orbit satellite and the Queqiao relay satellite can be used as the epitome of the development of Chinese satellite in the past decade. Looking around the world, space technology represented by satellite antennas has also developed rapidly in recent years, providing strong technical support for communication relay, deep space detection, meteorological observation and other applications [1]. Since the antenna gain is proportional to the square of the aperture [2], in order to capture small power signals and meet the demand of high gain and high coverage, large aperture antenna with feature size of tens of meters [3, 4] was urgently needed. For example, the aperture of Hoop Reflector Antenna proposed by Harris Company has reached 22 m, and the maximum deployed aperture of the starlight cover (Exo-S Shade) proposed by the JPL can reach 34 m [5]. However, the maximum aperture of the payload in current rocket is about 5 m. The contradiction between the rocket limitation and the increasing aperture of the satellite antenna makes the antenna possess the characteristics of scalability [6]. That is, the antenna is folded in the rocket while the antenna unfolds in orbit.

Over the past four decades, deployable satellite antennas have been proposed in a variety of ways. According to configurations and deployment ways, they can be divided into three basic types: rigid surface deployable antenna, inflatable antenna and deployable mesh antenna [7]. The rigid surface deployable antenna [8] is composed of some approximate rigid surfaces, and the precision of the surface is quite high, but the structure is bulky and the stowed volume is large. Hence it is difficult for antennas with large aperture. The inflatable antenna [9, 10] belongs to a kind of inflatable film structures with high package efficiency. However, the precision of the surface is poor, which is restricted by the material, process and other factors, resulting in that it still remains in the experimental stage. As shown in Fig. 1.1, a deployable mesh antenna [11–13] is made of flexible mesh, which is light and easy to unfold and capable of combining with the support structure, such as umbrella mesh antenna represented by and folded ribs [14] and a ring mesh antenna supported by the ring truss [15, 16], etc. Mechanically, the umbrella antenna [17, 18] is equivalent to a cantilever beam with radial radiation, while the ring mesh antenna [19] is similar to a closed thin shell. In contrast, the ring mesh antenna has a high specific stiffness and a high package ratio, which is an ideal structure for realizing large aperture antennas.

The mesh antenna Astromesh [19] was proposed by Northrop Grumman Corporation, and it was first successfully applied to communications satellites Thuraya in May 2000, and subsequently to MBSat, Inmarsat 4, Alphasat and recent SMAP projects, with a success rate of 100% in the current public literature and reports. As shown in Fig. 1.2, the mesh antenna is composed of two parts: a

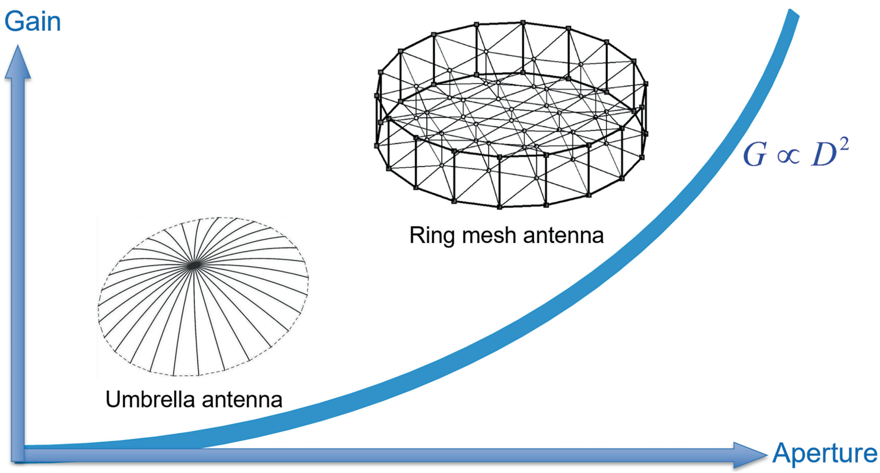

Fig. 1.1 Different types of deployable mesh antennas, where G denotes gain and D signifies aperture

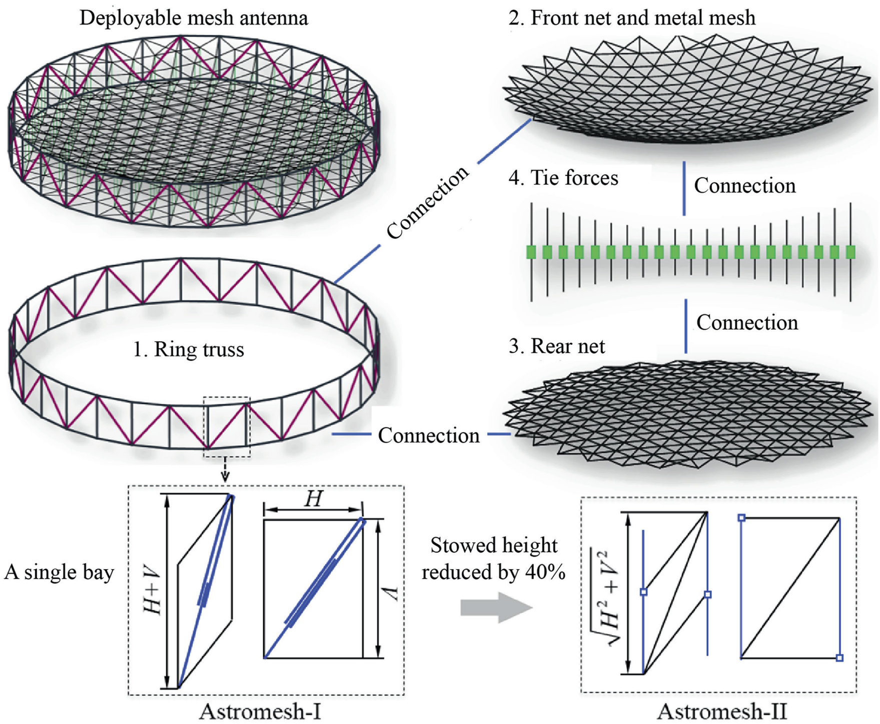

Fig. 1.2 Deployable mesh antennas: Astromesh-I and Astromesh-II

deployable ring truss and cable networks [20]. If the members of the ring truss are considered as rigid parts, the ring truss can be regarded as a deployable mechanism with a single degree of freedom [21, 22] which is unfolded by motors. The cable networks consist of a front net, a rear net, a metal mesh attached to the front net (used to receive and send electromagnetic signals, not shown in the diagram), and a tension tie spring (also known as a tension array) between the front and rear net [23]. When the antenna is fully unfolded, the tie springs will tighten the nodes corresponding to the front net and the rear net, thus maintaining the parabolic configuration and the necessary overall stiffness of the structure.

Figure 1.2 shows two deployment forms of the ring truss, including Astromesh-I [24] and Astromesh-II [25]. Both are composed of similar bays, each of which has two longerons with length H, two battens with length V and a diagonal. For Astromesh-I, each diagonal contains two telescope tubes, and longerons and tubes are hinged with battens. Elongating the diagonals can fold the ring truss, and vice versa. When fully folded, battens are co-linear with longerons, hence the stowed height is $H + V$. The revolute joints of adjacent bays are synchronized by a pair of interlocking gears.

However, Astromesh-II has a different unfolding mechanism, in which each diagonal is in one piece. One end of a longeron hinges with a batten, and the other end connects with the other batten through a translational joint. The translational joints of adjacent bays are synchronized through particularly designed cable-pulley systems. When fully folded, the stowed height is the diagonal length. Among these two models, Astromesh-II has a more complex synchronization mechanism. Nevertheless, owing to the lower stowed height, it is preferred by large mesh antennas for saving storage space. Astromesh-II will become an important choice of large satellite antenna in the future and is also the research object of this thesis.

Whether the antenna can be successfully deployed directly determines the success or failure of the whole satellite mission. Because of the complexity of antenna mechanism and the influence of gravity, it is difficult to give accurate and complete description according to ground experiments. Dynamic simulation provides technical support for antenna design and in-orbit behavior prediction [12, 26–28]. Different from the Astromesh-I [29–32], the Astromesh-II has adopted a new deployment mechanism which lacks a systematic and in-depth understanding. In the antenna design stage, the first problem is to design the proper synchronization mechanism to ensure the synchronous deployment of each bay of the ring truss, and the multiscale characteristics of the synchronization mechanism become the bottleneck restricting the dynamics simulation of antenna. In addition, it is necessary to evaluate the influence of the synchronization mechanism on the antenna deployment dynamics, such as the driving force by motor and the component loads and other parameters. On this basis, it is also necessary to find out the possible problems in unfolding process, find out unreasonable aspects in the current design, and further improve or propose new designs.

As shown in Fig. 1.2, after the antenna is fully deployed, the tie springs make both the front and rear net taut. The metal mesh is attached to the front net and the parabolic surface is fitted with triangular surfaces [33]. The electromagnetic transmitter/receiver located at the focus of the parabolic surface. Compared with rigid surfaces, the flexibility of cable networks leads to a great challenge in realizing parabolic configuration with high precision. It usually requires that the root mean square (RMS) error of the surface can be controlled within the order of millimeters, and that the profile error cannot change with the increase of the diameter of the antenna [34]. As a quantitative example, an S-band mission with a frequency of 4.0 GHz (wavelength 75 mm) requires a shape error as small as 1.5 mm, regardless of the aperture size: for instance, 6 m or 30 m [35, 36]. Therefore, investigations on factors and methods that can affect and/or improve the shape precision are of great concern.

To sum up, there are two core tasks for the deployable mesh antenna: The first is to make the antenna deploy on orbit successfully, which involves determining whether the motor driving force is enough to ensure the antenna is fully deployed, and whether the strength of each component of the antenna is enough to withstand the load during unfolding process. The second is to form a high-precision paraboloid to send and receive electromagnetic signals after the antenna is fully deployed. The core problem is how to achieve a paraboloidal surface with required precision in orbit.

1.2 Current Research and Unresolved Issues

1.2.1 *Design of Deployable Structures*

Driven by motors, the ring truss realizes the transition from the stowed state to the deployed state. Since the motors are located on a certain bay of the ring truss, in order to ensure that each bay of the ring truss can be deployed, the ring truss should have a single degree of freedom if each component of the ring truss can be regarded as rigid. At this time, it is necessary to introduce a specific design to ensure the synchronization of each bay of the ring truss, which is called the synchronization mechanism. The mesh antennas including Astromesh-I and Astromesh-II adopt different synchronization mechanisms as shown in Fig. 1.3. For Astromesh-I, each diagonal contains a pair of telescope tubes, longerons and battens. Reeling-in the driving cable by motor can shorten the diagonals, resulting in unfolding the ring truss. At the same time, a pair of synchronous gears is introduced between the adjacent two bays to ensure that the rotation angles of the adjacent two bays are equal. An asynchronous unfolding process from the near-motor side to the far-motor side in sequence occurs during deployment. For Astromesh-II, the synchronization mechanism changes from the synchronous gears to synchronization cable-pulley systems, which aim to ensure the same displacement between the two adjacent translational joints along battens. Taking a single bay as an example, there are two translational joints, and the original degree of freedom is two. When the left slider moves down after using the synchronization cable-pulley system, the synchronization cable will pull the right slider up; when the left slider moves up, the synchronization cable will pull the right slider down. Hence the displacement of the two adjacent sliders is mutually restricted. The goal is to make the ring truss into a system with single degree of freedom.

Theoretically, if all components of the ring truss are considered as rigid bodies, the synchronous gears ensure that the ring truss of Astromesh-I has only one degree

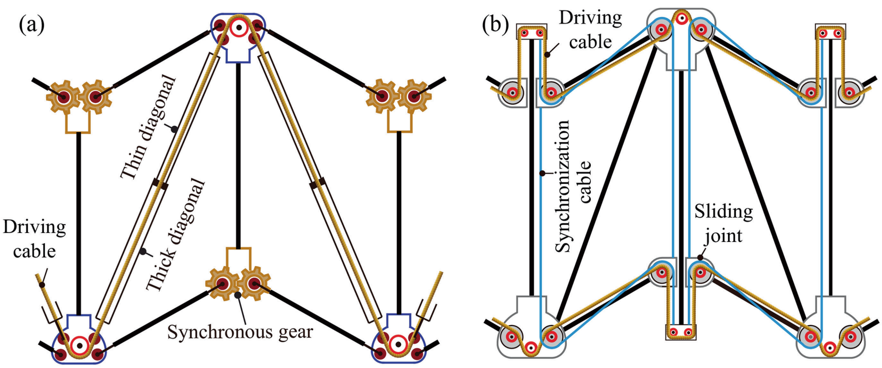

Fig. 1.3 Synchronization mechanism: (**a**) Astromesh-I with synchronous gears; (**b**) Astromesh-II with synchronization cable-pulley system

of freedom, and each bay will be completely synchronized. In fact, the flexibility of the truss and the tension decay of driving cables through pulleys cause an asynchronous deployment. The ground unfolding experiment of Astromesh-I shows that the bays deploy from the near-motor side to the far-motor side in sequence. Specifically, the bays near the motors begin to latch at first, and the bays far from the motors latch at last. Considering that the flexibility of the ring truss becomes remarkable with the increase of antenna diameter, the rigid assumption of the ring truss can no longer correctly describe the dynamic behavior of deployment. Peng Yun [37], Li Pei [38], Liu [39, 40] and others have established the flexible dynamic models of Astromesh-I respectively. The simulation results showed the asynchronization of deployment.

Current research results show that the asynchronous deployment of Astromesh-I [41] has a significant effect on the deployment dynamics, such as the loads of components (the bending moments of the truss mainly), and the driving force of motors. Compared with the synchronous gears in Astromesh-I, the synchronization cable-pulley systems used in Astromesh-II have a more complex design to ensure synchronization. For Astromesh-II, it is necessary to evaluate the effect of synchronization mechanism on deployment dynamics. On this basis, problems and unreasonable designs can be found out, and new designs and improvements can be further proposed.

1.2.2 Modeling and Simulation of Deployable Antennas

Recently, the rapid development of flexible multibody system dynamics [42, 43], especially the proposed flexible element with large deformation, provides a powerful tool for modeling and simulation of deployment dynamics of deployable antennas [44]. For modeling methods, multibody system dynamics can be divided into three categories: the floating coordinate formulation, the absolute node coordinate formulation (ANCF), and the geometric accurate formulation. The floating coordinate method [45] is to establish a floating coordinate frame attached on the flexible body, which decomposes the motion of the flexible body into the implicated movement of the floating frame (large scale of the rigid translational and rotational motion) and the small elastic deformation relative to the floating frame, which is suitable for the system with small deformation. The absolute node coordinate formulation [46, 47] was proposed by Shabana, in which the movement and deformation of the flexible body are expressed by the spatial coordinates and gradient coordinates of the element nodes relative to the inertial coordinate frame. On this basis, finite elements including beam, plate, shell and solid are developed with high precision of displacement description. The geometric accurate formulation was first proposed by Simo in the 1990s [48, 49]. For calculation, the curvature is used to describe the deformation of beams and shells in three-dimensional space, and both the rotation and displacement are interpolated independently. Since the beam and shell are mainly subjected to bending load in most cases, it is more suitable to describe the three-dimensional bending deformation of beams and shells.

Jiali Tang [50] proposed a time-varying flexible beam element based on the absolute node coordinate formulation. Both the absolute coordinate and slope of the node are used to describe the configuration of the element, and the influence of the mass flow at borders is considered. Lei Yu [51] established a unified solution framework of flexible multibody dynamics. It provides a complete set of modeling methods for large rotating and deformed flexible bodies by combining one-dimensional cable/beam element, two-dimensional plate/shell element and three-dimensional solid element with existing multibody system algorithms according to the first class of Lagrange equations. Qiang Tian [52] used the method of absolute node coordinates formulation to study the multibody systems with kinematic joints considering the clearance and friction (including revolute joint and spherical joint), and conducted the sensitivity analysis. Difeng Hong [53] proposed the Eulerian Bernoulli beam element described by arbitrary Lagrangian-Eulerian description, and the sliding joint along one-dimensional flexible medium was established. Zhihua Zhao [54] developed the method of geometric accurate beam and shell elements based on rotational vector description. Pei Li [38] proposed a recursive algorithm based on static condensation and multi-layer region decomposition, and the MPI parallel technique was used to solve the dynamic equations of largescale multibody systems efficiently. Yun Peng [37] proposed a variable length cable element with arbitrary Lagrangian-Eulerian description, the material coordinates were introduced into the generalized coordinates of the cable element. Based on this, a simplified modeling method of the cable-pulley system was proposed. In order to improve the computational efficiency, Li Pei et al. [38] conducted the simulation of the deployment of antenna by using parallel calculation, analyzed the influence of cable pretension on the deployment, and discussed the main reasons that caused the asynchronization of the deployment.

A series of modeling and simulation studies on the Astromesh-I have been carried out by Mengliang Zhao, Fulin Guan, etc. [55, 56], in which the dynamic equation of the deployment of the ring truss was established by the generalized inverse matrix method, the deployment of the antenna was analyzed, and the mechanism of friction in the deployment process was studied. Chaohui Qi [57] studied the influence of the parameters of the pulleys on deployment. The relationship between the deployment speed of the antenna and the reel-in velocity of driving cables by motors was given from the kinematics point of view, and the deployment process of the antenna is controlled by controlling the reel-in velocity of the driving cables by motors. Based on the multibody dynamics method, Tuanjie Li [58] established the dynamic model of Astromesh-I, obtained the change of the driving force during deployment, and studied the effects of torsion stiffness of springs and pretension of webs on deployment. Yun Peng [31] established the flexible multibody dynamic model of Astromesh-I, and simulation results showed an asynchronous deployment, which was validated by the on-ground experiment. On this basis, the influences of the asynchronous deployment on the driving force by motors and the load of the ring truss were systematically analyzed. In order to improve the computational efficiency, Pei Li [38] simulated the whole process of the deployment with parallel calculation, analyzed the influence of pretension of cables on deployment, and discussed the main reasons for the asynchronous deployment of the ring truss.

For the cable-pulley systems in Astromesh-I, if the cable-pulley system is modeled by traditional contact method, it requires the element length to be about one tenth of the pulley size for fitting the pulley curvature, resulting in large amount of generalized coordinates and contact detection, as shown in Fig. 1.4. Therefore, the calculation efficiency is too low to fulfill an unfolding simulation of a mesh antenna. Peng et al. [59] proposed an efficient method, which avoided contact detection based on variable-length cable elements with Arbitrary Lagrangian–Eulerian (ALE) formulation, as shown in Fig. 1.5. However, it actually bypasses rather than solves the multiscale problem by treating pulleys as dimensionless points, which is only suitable when the pulley size does not matter, such as the case in Astromesh-I.

Nevertheless, the pulley size is crucial in the synchronization mechanisms of Astromesh-II, since it affects the synchronization conditions of adjacent bays. Therefore, the multiscale nature of the cable-pulley systems must be exactly modeled, and the effects of synchronization on cable-pulley systems on deployment dynamics can be investigated based on this, which will be one of the contents of this thesis.

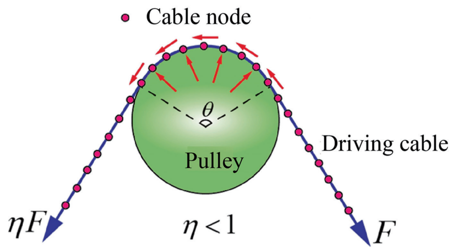

Fig. 1.4 Contact modeling method of the cable-pulley system, where F denotes the cable tension and η signifies the coefficient of tension decay of the cable passing through the pulley

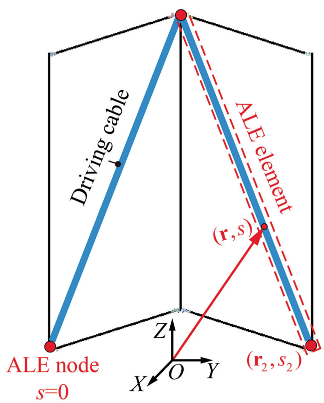

Fig. 1.5 Simplified ALE Modeling Method for Cable-Pulley Systems, where $\boldsymbol{r}$ represents the position coordinate and s denotes the material coordinate

1.2.3 Design of Cable Networks

A mesh antenna comprises a supporting truss and a pair of mirror cable networks mutually tensioned by low-stiffness tie springs. The cable networks consist of a front net, a rear net, a metal mesh attached to the front net, and a tension tie spring (also known as a tension array) between the front and rear net. When the antenna is fully deployed, the tension array will tighten the nodes corresponding to the front net and the rear net, thus maintaining the parabolic configuration and the necessary overall stiffness of the structure. The metal mesh is attached to the front net and the parabolic surface is fitted with triangular surfaces. The electromagnetic transmitter/receiver is located at the focus of the parabolic surface. The quantitative relationship between parabolic gain and shape error [60] as

$$\frac{G}{G_0} = \exp\left[-\left(\frac{4\pi e}{\lambda}\right)^2\right] \tag{1.1}$$

in which G is the gain of the mesh surface, G_0 is the standard parabolic gain, λ is the electromagnetic wave length, and e is the root mean square (RMS) error of the mesh surface. Applications demand surface errors smaller than 1/50th of the wavelength [35, 36]. Therefore, it is a great challenge to achieve a parabolic surface with high precision. The design of cable networks involves two aspects: The first is the design of topology, including the number of network surface nodes and the corresponding connection; The second is the geometric design of cable segments, or the coordinates of cable nodes on the net.

First, at the topological level, Calladine [61, 62] and Tibert [63] proposed that after the mesh antenna is completely unfolded, the whole system including the cable networks and the ring truss should be a statically determinate structure, that is, the degree of freedom of the whole system is exactly 0:

$$0 = 3(n+b) - (b+c+b+3) = 3n + b - c - 3 \tag{1.2}$$

in which b is the number of the bars (the number of bar nodes); n is the number of the cable nodes (the number of tie springs); c is the number of the cables. For the statically determinate design, the shape of the cable network is determined solely by the lengths of the structure members with a given topology. Hence, if the length error is negligible, the cable nodes should be located on the ideal surface. Figure 1.6 shows four webs with different topologies when the bar nodes $b = 30$, in which p represents the number of meshes along the radius. Theoretically, the tessellation error decreases with the increase in the meshes. However, dense mesh leads to the increase in the mass of the cable networks and more errors in the cable lengths. Therefore, a simplified topology should be adopted on the premise of satisfying the required shape precision.

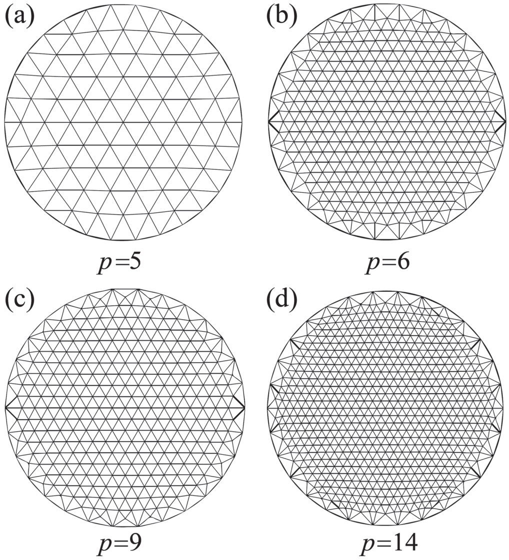

Fig. 1.6 Designs of statically determinate structure with different topologies: the number of meshes increases from (**a**) to (**d**)

Secondly, in the geometrical design of the cable networks, lots of shape finding methods have been proposed in the opening literature [64]. Shek [65] and Linkwitz [66] proposed the force density method, in which the force density is defined as the ratio of cable tension to its length, and the coordinates of each node can be obtained according to the force density of each cable. The advantage of force density method is that the position coordinates of each node can be solved by linear equilibrium equations instead of iteration. Based on the force density method, the minimum length configuration was obtained by Tibert [63, 67] on the premise of equal force density. Recently, the research on the geometric design of cable networks by optimization has been a hot topic. Morterolle et al. [68] proposed the improved force density method to ensure the uniform distribution of the mesh tension. Based on the finite element model of the cable networks, Jiejian Di [69], Dongwu Yang [70], Rui Yang [23], Jingli Du et al. [71] adopted optimization algorithms including genetic algorithm, inverse iteration method, sequential quadratic programming method and minimal norm method to improve the accuracy of the mesh surface. Pei Li [72] considered the influence of flexible deformation of ring truss in the process of shape finding of the cable networks. In addition, studies have been carried out on the influence of length error on shape precision [73–75], and relevant attempts have also been made to adjust the length of several cable segments to improve the shape precision [76, 77] and the electromagnetic performance [78–84].

At present, most studies focus on the geometrical design of the cable networks when the topology is given, and the influences of length error on shape precision are investigated. However, the influence of the tie forces on shape precision cannot be ignored. If the tie forces are not appropriate or there exist large force errors of the tie forces, part of the cable networks may be slack, resulting in remarkable shape